



# Fuzzy logic based computational model for speckle noise removal in ultrasound images

Muhammad Nadeem<sup>1</sup> · Ayyaz Hussain<sup>1</sup> · Asim Munir<sup>1</sup>

Received: 18 May 2018 / Revised: 23 November 2018 / Accepted: 15 January 2019 /

Published online: 29 January 2019

© Springer Science+Business Media, LLC, part of Springer Nature 2019

## Abstract

High level of uncertainty is always present due to impulsive noise in ultrasonic images, which may put negative effect on image interpretation, quantitative measurement and diagnostic purposes. In order to deal with this uncertainty, fuzzy modelling is being used which is very helpful in distinguishing noise from edges and other critical details present in the image. In this study, a novel fuzzy logic based non-local mean filter is proposed to model the speckle noise and to restore the degraded image using Fuzzy Uncertainty Modelling (FUM), smoothed by local statistic based information while preserving the image details for low and highly speckled ultrasound images. Proposed denoising technique acquires the local parameters to find distinct “*similar and non-similar*” non-local regions using FUM. These homogenous regions are first smoothed through local statistical information and then used to restore the selected noisy pixels using fuzzy logic based noise removal process. The study evaluates the performance of the proposed technique on different real and simulated data sets, and compares the numerical values with existing state of art filters using standard well known global quantitative measure like signal to noise ratio (SNR) and a local error measure – structural similarity index measure (SSIM). Visual and quantitative results demonstrate that the proposed technique outperforms the existing state of the art filters in removing speckle noise while preserving the edges and other important details present in the image.

**Keywords** Ultrasound imaging · Image despeckling · Image restoration · Fuzzy uncertainty modelling · Non local mean · Fuzzy similarity based non-local-mean · Local statistics

---

✉ Ayyaz Hussain  
ayyaz.hussain@iiu.edu.pk

Muhammad Nadeem  
nadeem@iiu.edu.pk

Asim Munir  
asim@iiu.edu.pk

<sup>1</sup> International Islamic University, Islamabad, Pakistan

# 1 Introduction

Unlike other non-invasive imaging techniques, ultrasound (US) images are playing vital role in medical diagnostics to visualize and examine the internal human body structures due to its portability, substantially cost effective nature and harmless ionizing radiations. During acquisition or transmission process these images may corrupt by additive and multiplicative speckle noise [7, 11]. Speckle is a granular noise that inherently degrades the quality of the image resulting in complications for the detection of small edges and other textural details. Image denoising is a required pre-processing step for every image processing and computer vision task. It helps in extracting reliable and accurate information using segmentation, feature extraction and classification purposes from the ultrasound image. In computer vision, image denoising can help to enhance the appearance model and facilitate the object detection and tracking accuracy [19–21]. Current study addresses the multiplicative type of uncertainty present in almost every ultrasound medical image.

## 1.1 Speckle reduction techniques

The speckle in US image is often considered as undesirable and several noise removal techniques have been proposed considering the signal dependent nature of the speckle intensity. In this section, we present a classification of standard adaptive filters and other methods for speckle reduction.

### 1.1.1 Standard adaptive techniques

Medical image smoothing may cause the blurring effect while edge sharpening may lead to noise amplification [25]. In most of the existing denoising methods, filters are applied on the entire image rather than applied on the noisy part of the image only. As a result, noise free pixels are also changed which destroys the image content considerably and produce false artifacts. In order to despeckle the images considerably, specific filters have been designed both in spatial and transformed domains [26]. Existing methods use a variety of adaptive local statistical spatial filters such as average, median, wiener, Lee, Frost and Kuan filters [9, 18, 22]. These filters provide visually enhanced image to make an accurate diagnosis by reducing speckle noise effectively, but quantitative analysis show that they do not precisely preserve the important features of the required data such as thin lines, edges and anatomical boundaries in the image.

### 1.1.2 Partial differential equations (PDE) based methods

A balance between the preservation of useful diagnostic information and noise suppression is the main goal of computer-aided diagnosis (CAD). To preserve the fine edges and suppress speckle in images, Anisotropic Diffusion (AD) filter [1] and its variants Speckle Reducing AD (SRAD) filter [35], Oriented SRAD filter [17] are used. These filters works well for regional features preservation but for point and linear feature characterization, they need to be corrected. Due to iterative nature of these filters, some important detail may disappear from the image which is the major drawback of this technique. To preserve the minor details, Squeeze Box (SB) filter [31] is proposed as a preprocessing step for enhancing contrast of B-mode images by compressing the pixel distribution range to some limit in homogeneous

regions while preserving the average mean values of distinct regions of the image by using local statistical functions. To address the speckle noise in the image, other transform domain denoising methods are also used. However almost all methods generally produce unwanted or false artifacts in the image which can lead to false diagnosis. So more robust and accurate detail preserving despeckling filters are in need and being sought. The despeckling methods mentioned above are based on local statistical information. The pixels in the image are highly correlated and the noise is generally independent, so to simply averaging these pixels yield considerably noise reduction, but makes the edges more blurred.

### 1.1.3 Switching scheme based methods

A “*Switching scheme concept*” is introduced in [29] that improves the speckle noise detection process without affecting the image details. This technique first detects the noisy pixels from the image then only these pixels are subjected to the noise removal process leaving the noise free pixels unchanged. Most of the newly proposed filters are based on this switching scheme based approach.

### 1.1.4 Deep learning (DL) based methods

Over the recent years, DL [16, 24] has had a remarkable impact on various fields in science. It has led to substantial improvements in image restoration, image segmentation, image detection and recognition, image registration and speech recognition. Obviously this technology is also highly relevant for medical imaging. There have been several attempts to handle the denoising problem by DL algorithms [10, 12, 15, 23, 27, 36]. Despite of the promising results, DL-approach has some shortcomings as well. One of the biggest hurdles of DL research in medical imaging is the data hungry nature of the DL algorithms. It needs to be trained with large sets of labelled data. The larger the training data set, the better the performance of the algorithm. Secondly, it is computationally very expensive which restrict it to be used in real-time scenario. Furthermore, a DL algorithm requires many tuning parameters to properly train the model that makes it difficult to configure. The complexity of the hidden layers of DL algorithm hinder to interpret the results or to understand the algorithm mechanism.

### 1.1.5 Non local mean (NLM) based methods

Non Local Mean filtering [2, 6] is a non-local technique in which only selected regions are used to model the uncertainty present in the image. NLM analyzes the data in large and collects the observations from the whole image looking for similar features. This technique removes the noise cleanly preserving the edges and other fine details. This filter uses similar local regions within the image to calculate the weights of the pixels contain noise. NLM filter is best to restore periodic or textured image. Due to this property, NLM filter has proven to be an effective and efficient restoration technique and has been used by many researchers to despeckle ultrasound images. OB-NLM (Optimized Bayesian NLM) [8] filter uses a Bayesian framework is also adopted to address speckle noise. The performance of the NLM filters is inversely related to the degree of noise in the image. As the noise increase, the NLM and its variants start to produce blurring effect within the image which decreases its quality. Therefore, NLMLS (Non local mean filter combined with local statistics) [34] is proposed that combines the best features of local statistics and NLM filter and effectively reduce the speckle noise in

the ultrasound images. The noisy regions input to the NLM are first smoothed based on the local statistical features which are then used to compute the weights for the NLM. Results show significant improvement in the quality of despeckled ultrasound image. Another hybrid algorithm for making impulse free ultrasonic image [30] uses a three step non iterative process to despeckle the ultrasound images. The local statistical information of the image is obtained and is used to reduce speckle noise in first step followed by applying improved SRBF – “*Speckle Reducing Bilateral Filter*” to further lessen the speckle noise. In third step, NLM filter is applied to reconstruct the diffused edges as a post processing technique.

### 1.1.6 NLM based fuzzy mechanism

NLM filters using fuzzy similarity mechanism have also been proposed recently for eliminating random valued impulse noise, multiplicative speckle noise and rician noise from the medical images [5, 28, 33]. These methods use fuzzy logic to identify the degree of similarity between multiple non-local regions present around the noisy pixel.

In this study, a novel filter is proposed that uses local statistics [4] based information for uncertainty modeling based on a computational model – Fuzzy Uncertainty Modelling (FUM) for speckle noise reduction in ultrasound images. The proposed technique uses the concept of fuzzy logic based uncertainty modelling that analyzes the non-local regions to identify the most “*similar*” ones present in the non-local region of the corrupted pixel. These regions are smoothed by applying local statistics before forwarding to fuzzy restoration mechanism. This filter creates a balance between the degree of noise removal and edge preservation in an effective way.

Extensive experimentation is performed on synthetic, B-mode simulated and real ultrasonic images to evaluate the performance of the proposed technique both qualitatively and quantitatively and the results are compared with standard state of the art filters (SRAD [35], SBF [31], NLM [6], OBNNLM [8] and NLMLS [34]). Comparative analysis of the results confirmed that the proposed denoising filter performs better than the existing techniques in suppressing the multiplicative noise present in the ultrasound medical images while preserving the edges and fine details.

## 1.2 Contributions

Major contributions of the proposed technique include:

- It acquires the local statistical parameters to find distinct non-local homogenous regions using FUM.
- FUM is used to make suitable tradeoff between two contradictive objectives, image restoration and structural preservation.
- Proposed fuzzy based computational model gives superior performance both in terms of despeckling and detail preservation.
- Model is computationally efficient due of less number of multiplications and additions as only similar non local regions of the image will estimate the restored value of the noisy pixel.

The remainder of this article is organized as follows: Section 2 presents speckle noise model, proposed methodology, explanation of noise estimation and removal process. Experimental

setup, results and comparative performance analysis of proposed technique with traditional state of the art approaches is described in Section 3. Finally conclusions and future directions are presented in Section 4.

## 2 Methodology

The main objective of the proposed technique is to estimate and eliminate multiplicative type of speckle noise from ultrasound medical images while preserving the high-frequency contents that are the edges and fine details. The proposed fuzzy logic and local statistics based NLM technique comprises of five modules namely modelling the speckle noise, preprocessing, fuzzy uncertainty modelling, local statistics and fuzzy restoration mechanism. In [11] speckle noise is modeled as multiplicative one in nature. Parameters required for noise free pixel estimation is acquired in preprocessing module. In the fuzzy uncertainty modelling step, a fuzzy based classifier aids in finding the more “similar” non-local regions of the pixel under consideration. The selected local and non-local regions are smoothed by the local statistics. These processed regions are then used in the module of fuzzy restoration of the noisy pixel. Block diagram of the proposed technique is given in Fig. 1.

### 2.1 Speckle noise model

Mathematical model of the speckle noise given in (1) shows that the noise distribution in ultrasound medical image is signal-dependent and multiplicative in nature [11] and is given as under:

$$I^{noisy}(x) \approx I^{original}(x)\eta(x) \quad (1)$$

Original image is represented by  $I^{original}(x)$ ,  $x$  is the pixel location, the observed image with noise is represented by  $I^{noisy}(x)$  and  $\eta(x)$  specifies multiplicative noise component.

The following equation is obtained after applying log transformation to the mathematical model in (1):

$$\log(I^{noisy}(x)) \approx \log(I^{original}(x)) + \log(\eta(x)) \quad (2)$$

The general model of speckle noise is given in the following expression:

$$I^{noisy}(x) = I^{original}(x) + I^{original}(x)^r * \eta(x) \quad (3)$$

where factor  $r$  is attributed to the ultrasound acquisition device having Gaussian distribution with zero mean. In the ultrasound image study of B-mode, a good representation of ultrasound data is made by setting  $r$  equal to 0.5. The model shows that speckle noise is multiplicative when  $r$  is set to 1.

### 2.2 Pre-processing module

A smaller size of search window of radius  $R_{search}$  is convolved around a noisy  $pixel_i$ . Fuzzy logic based statistics criteria is used to find  $pixel_j$  similar to  $pixel_i$ .  $R_{similar}$  represent the radius of local and non-local windows  $W_i$  and  $W_j$  centered at  $pixel_i$  and  $pixel_j$  respectively. Similarity between  $pixel_i$  with all non-local neighbouring  $pixel_j$  is

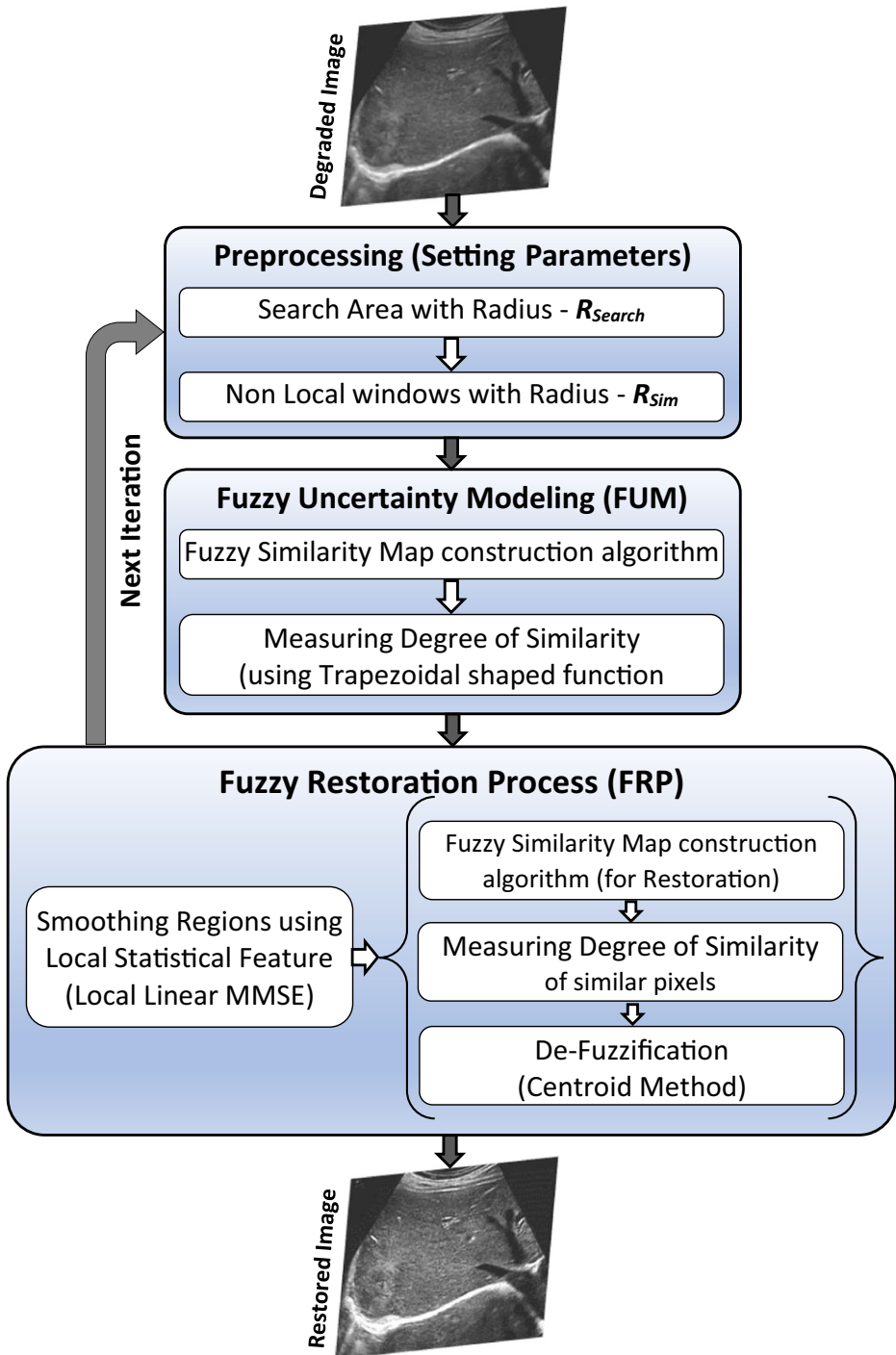


Fig. 1 Overview of the proposed filter-based framework

computed using region based comparison method. Detailed procedure is discussed in the coming sections.

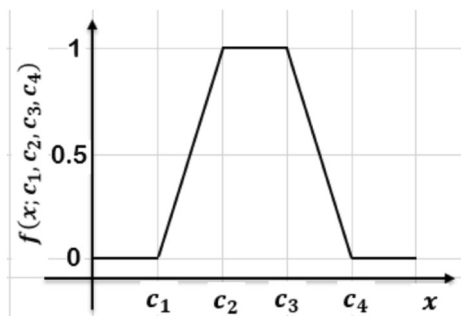
### 2.3 Fuzzy logic based computational model

In this phase, degree of similarity of window  $W_i$  with each non-local window  $W_j$  is measured using fuzzy logic based mechanism. A reasonably good noise free pixel can be approximated by looking for the similar pixels within the non-local neighborhood. Pixel values of the edges are very different than the other values of the region and normally isolate two regions of the image. To estimate noise free pixel using non-local neighbor, which are not the part of edge can deform the boundaries of neighboring regions. These deformed edges can misclassify certain disease in ultrasonic data. Detecting same patches/regions in the non-local neighborhood of the centered patch  $W_i$  is a challenging task due to higher degree of uncertainty present in the noisy ultrasound images. Fuzzy logic based mechanism is used to overcome these uncertainties and thus two fuzzy membership functions are formed. These functions use mean-ratio  $R_\mu$  and variance-ratio  $R_\delta$  of  $W_i$  and  $W_j$  patches to calculate the degree of similarity. These similarities are then combined to find the degree of similarity of the non-local window  $W_j$ . Higher the degree of membership, more is the similarity between the local and non-local region, however lower degree means that  $W_j$  belong to different region and therefore the pixels are discarded in the despeckling process. For fuzzy similarity mechanism trapezoidal shaped function is used as given in Eq. 4, and shown in Fig. 2.

$$f(x; c_1, c_2, c_3, c_4) = \begin{cases} 0 & \text{if } x \leq c_1 \\ \frac{x-c_1}{c_2-c_1} & \text{if } c_1 \leq x \leq c_2 \\ 1 & \text{if } c_2 \leq x \leq c_3 \\ \frac{c_4-x}{c_4-c_3} & \text{if } c_3 \leq x \leq c_4 \\ 0 & \text{if } c_4 \leq x \end{cases} \quad (4)$$

where  $x$  be a vector providing input to the trapezoidal function. Constants  $c_1, c_2, c_3$  and  $c_4$  are the scalar factors. Here  $c_1$  and  $c_4$  localize the base of the trapezoidal function,  $c_2$  and  $c_3$  forms the values of the top. The step-by-step process of these factors calculation and measuring the degree of similarity between the two input windows  $W_i$  and  $W_j$  is described in *Algorithm-1*. All the non-local regions similar to local regions are identified at this stage.

Fig. 2 Trapezoidal shaped membership function



*Algorithm-1* takes local and non-local windows  $W_i$  and  $W_j$  as input along with three constants, *mean-membership*  $\mu_c$ , *variance-membership*  $\sigma_c^2$  and *similarity-threshold*  $S_t$ . The values of constants and threshold depend upon the means and variances of similar and non-similar regions. In case of speckle noise removal, these values are set experimentally by analyzing ratios of mean  $\gamma_\mu$  and variance  $\gamma_{\sigma^2}$  defined in Section-4. Constants  $\mu_c$  and  $\sigma_c^2$  are used to set constants  $c_1, c_2, c_3, c_4$  and construct two fuzzy membership functions. Similarity threshold  $S_t$  has been used to classify the similar and non-similar regions. Regions having degree of membership greater than or equal to  $S_t$  are considered similar and are used by the fuzzy restoration mechanism, however non-similar patches are simply ignored. Selection of similarity threshold has been made experimentally, value with best results has been given in experimental results section.

Algorithm-1: Fuzzy Logic based Computational Model [32]

<b>Input:</b>	Local-Window " $W_i$ ", Non-Local window " $W_j$ ", constant for Mean-Membership " $\mu_c$ ", constant for Variance-Membership " $\sigma_c^2$ " and Similarity-Threshold " $S_t$ "
<b>Output:</b>	Decision: Windows are " <i>Similar</i> " or " <i>Not-Similar</i> "
<b>Begin</b>	
1.	Find mean – $\mu_i$ and variance – $\sigma_i^2$ of $W_i$
2.	Find mean – $\mu_j$ and variance – $\sigma_j^2$ of $W_j$
3.	Calculate ratio of means – $\gamma_\mu$ of $W_i$ and $W_j$ , i.e, $\gamma_\mu = \mu_j / \mu_i$
4.	Calculate ratio of variances – $\gamma_{\sigma^2}$ of $W_i$ and $W_j$ , i.e, $\gamma_{\sigma^2} = \sigma_j^2 / \sigma_i^2$
5.	Calculate degree of membership – $S_\mu$ for $\gamma_\mu$ $x = \gamma_\mu, a = 0, b = \mu_c, c = 1/b, d = 1.1 \times c$ $S_\mu = f(x; a, b, c, d)$
6.	Calculate degree of membership – $S_{\sigma^2}$ for $\gamma_{\sigma^2}$ $x = \gamma_{\sigma^2}, a = 0, b = \sigma_c^2, c = 1/b, d = 1.1 \times c$ $S_{\sigma^2} = f(x; a, b, c, d)$
7.	Find the Similarity decision: IF ( $S_\mu \geq S_t$ ) and ( $S_{\sigma^2} \geq S_t$ ) then Windows are " <i>Similar</i> " ELSE Windows are " <i>Non-Similar</i> " ENDIF
<b>End</b>	

### 2.4 Noise estimation using local statistics

Most similar regions  $W_j$  identified in the previous phase are first smoothed using local statistics based noise estimation, then they are subjected to fuzzy restoration mechanism for restoration. For the estimation of noise-free region  $f(x)$ , Local Linear Minimum Mean Square Error (LLMMSE) [18, 34] is used and is given by:

$$\hat{I}_{LLMMSE}(x) = E(I(x)) + \frac{\delta_I^2(x)}{\delta_N^2(x)} [N(x) - E(N(x))] \tag{5}$$

where  $\hat{I}_{LLMMSE}(x)$  is the estimation of noise free image  $I(x)$ ;  $\delta_I^2(x)$  and  $\delta_N^2(x)$  are the variances of  $I(x)$  and noisy image  $N(x)$ .  $E(I(x))$  and  $E(N(x))$  are the expectations of ideal image  $I(x)$  and input noisy patch  $N(x)$  respectively. The values are calculated as described in [18].



### 2.5 Fuzzy restoration mechanism

Restored value of a noisy pixel  $pixel_i$  is calculated in this phase after processing the non-local similar patches with local statistics. Similar pixels have identical statistical properties between them. The degree of similarity of the distinct “local and non-local” regions are computed using Euclidean distance. Regions having low value have higher contribution in the noise estimation process and vice versa. Gaussian shaped fuzzy membership function with zero mean ( $\mu = 0$ ) and estimated noise variance ( $\delta^2$ ) is used to find the involvement of non-local region  $W_j$ .

$$weight(d_{ij}; \delta, \mu) = e^{-\frac{(d_{ij}-\mu)^2}{2\delta^2}} \tag{6}$$

Euclidean distance  $d_{ij}$  among the local region ‘i’ and non-local region ‘j’ is given by:

$$d_{ij} = \|W_i - W_j\| \tag{7}$$

The central pixel of patch  $W_i$  is also given a weight that is the maximum of all non-local pixel’s weights. After weighting all pixels in the search area, estimated noise free value of  $pixel_i$  is calculated in defuzzification step using fuzzy centroid technique and is given as:

$$pixel_i = \frac{1.0}{\sum_{k=1}^n weight_k} \sum_{k=1}^n (pixel_k \times weight_k) \tag{8}$$

The value of  $pixel_i$  gives the estimated restored pixel,  $n$  represents the count for non-local similar region and local region.  $pixel_k$  is the value of central pixel of window  $W_k$  and  $weight_k$  is the weight allocated to the most similar pixel computed using Eq. 6.

### 3 Experimental results and discussion

Four different type of tests are carried out to assess the performance of proposed technique. Experiment-I uses the synthetic data in which noise of different levels is introduced manually. Simulated data is used in Experiments II and III in which the images are generated through B-mode method applied on ultra-sound simulation [3] and through Field II [13, 14] respectively. SNR and SSIM [32] metrics are computed to gauge the results of the test methods, given by:

$$SNR = 10 \log_{10} \frac{1}{N_x N_y} \frac{\sum_{i=0}^{N_x-1} \sum_{j=0}^{N_y-1} \hat{g}^2(i, j)}{MSE} \tag{9}$$

where,

$$MSE = \frac{1}{N_x N_y} \sum_{i=0}^{N_x-1} \sum_{j=0}^{N_y-1} [I(i, j) - \hat{g}(i, j)]^2 \tag{10}$$

$$SSIM(\hat{g}, I) = \frac{(2\mu_{\hat{g}}\mu_I + c_1)(2\sigma_{\hat{g}I} + c_2)}{(\mu_{\hat{g}}^2 + \mu_I^2 + c_1)(\sigma_{\hat{g}}^2 + \sigma_I^2 + c_2)} \tag{11}$$

In the above equations,  $I$  and  $\hat{g}$  represents the original and restored images respectively,  $\mu_I$  and  $\mu_{\hat{g}}$  are the means and  $\sigma_I^2$  and  $\sigma_{\hat{g}}^2$  are the variances of images  $I$  and  $\hat{g}$  respectively that are used to compute the covariance  $\sigma_{\hat{g}I}$  of images  $\hat{g}$  and  $I$ .  $c_1 = (k_1 L)^2$  and  $c_2 = (k_2 L)^2$  are two factors that stabilize the division with a low denominator. The dynamic range of the pixel values (255 for 8-bit grayscale image) is represented by  $L$ . The default values for  $k_1$  and  $k_2$  are set to 0.01 and 0.03 respectively.

Signal to Noise Ratio (SNR) is the assessment of signal from error compared to the background noise. Increased value of SNR means decreasing the background noise and corresponds to the good quality image. The SSIM index evaluates the resemblance between the original and reconstructed image and is premeditated to improve over conventional approaches, such as mean squared error (MSE), which has been proved to be inconsistent with human eye perception. Structural knowledge is the notion that the pixels exhibit sound interdependencies, specifically when these pixels are spatially adjacent. These dependencies carry essential information concerning the structure of the entities in the visual sight. When two images are entirely identical, the value of SSIM becomes maximum that is 1.

The proposed technique is compared with numerous state of the art filters using these numerical quality measures. The compared filters are SRAD [35], SBF [31], NLM [6], OBANLM [8] and NLMLS [34] which shows good performance over traditional filters like median, Lee, Frost and Kuan etc. During the experiments, the number of iterations of the SRAD is kept 500 and for the SBF filter, it is kept 15. The size of region of NLM, OBANLM and NLMLS and proposed filters is kept  $5 \times 5$ , search area for these filters is kept  $11 \times 11$ . The values of the constants in the proposed filter are set experimentally which are: Mean-Membership " $\mu_c$ " = 0.62, Variance-Membership " $\sigma_c^2$ " = 0.19 and Similarity-Threshold " $S_i$ " = 0.7.

### 3.1 Synthetic images (Experiment-I)

To assess the performance of the qualitative and quantitative measures, synthetic image shown in Fig. 3a is considered which includes an oval, cardioid, line, triangle and a rectangle. This image is contaminated with different levels of speckle noise ( $\sigma = 0.2, 0.4, 0.6$  and  $0.8$ ) for experimentation purposes. A noisy speckled image having variance  $\sigma = 0.6$  is shown in Fig. 3b. Restored images obtained after applying various denoised filters are depicted in Fig. 3c-h. It can be clearly seen in the denoised images with SRAD and SBF filters shown in Fig. 3c and d that significant noise is still present in the images and fine detail (edge) preservation is not properly maintained. In case of NLM and OBANLM filters, over-smoothing effect is clearly visible as shown in Fig. 3e and f. The performance of NLMLS filter is better than others but exhibits many artifacts as shown in Fig. 3g. Fig. 3h shows that speckle noise is efficiently reduced and the image retains the original texture well as compared to other state of the art filters.

For quantitative analysis and comparison, SNR and SSIM values of the comparative filters and proposed filter are calculated under different levels of speckle noise and are listed in Table 1. Fig. 4 shows the SNR based and SSIM based comparison of filters under different noise levels which shows that proposed filter has attained maximum SNR up to 75% noise ratio and has approximately equal SNR and SSIM value to NLMLS above 75% noise ratio. This shows that in terms of SNR and SSIM measures, the proposed filter is best and more effective to reduce the speckle noise for synthetic images.

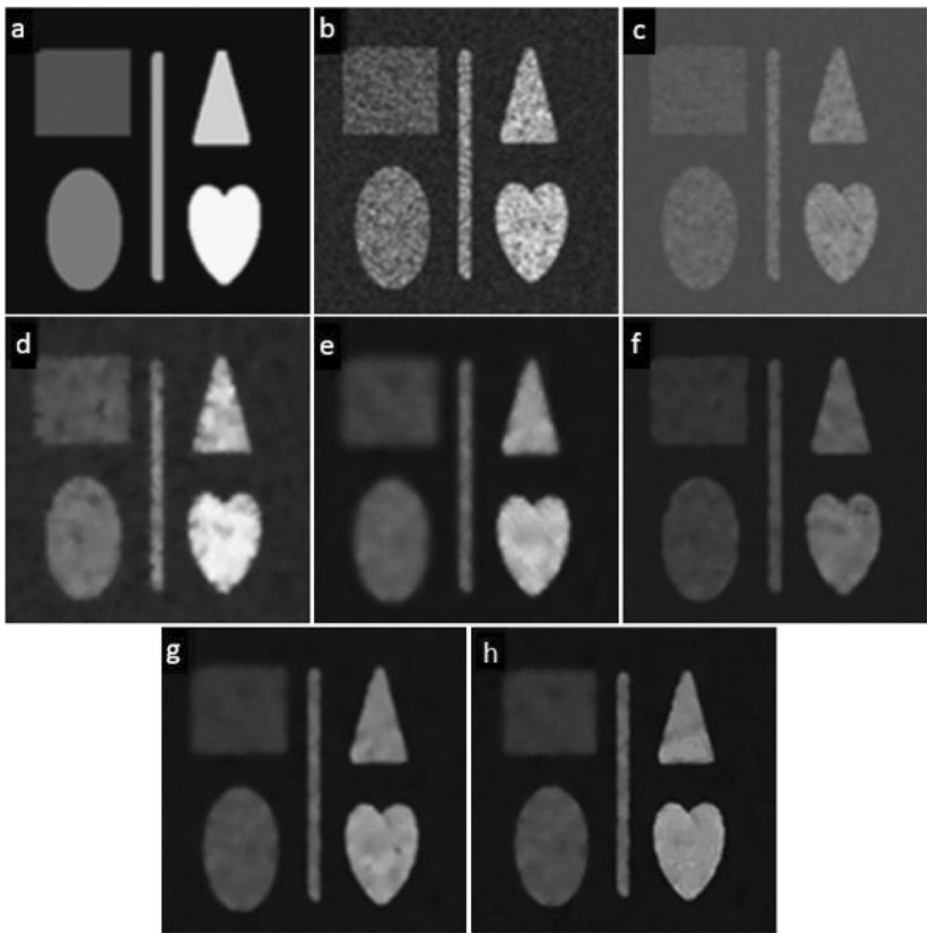


**Fig. 3** Denoised images obtained from different filters: **a** Original Synthetic image **b** Speckled image with noise  $\delta = 0.6$  **c** SRAD **d** SBF **e** NLM **f** OBANLM **g** NLMLS **h** Proposed filter

**Table 1** Comparison of SNR (db) and SSIM of different denoising filters on synthetic images contaminated with different levels of speckle noise

Method	SNR				SSIM			
	0.2	0.4	0.6	0.8	0.2	0.4	0.6	0.8
Noisy image	17.2	11.3	8.3	6.2	0.57	0.31	0.22	0.15
SRAD [9]	28.1	21.9	13.1	8.9	0.95	0.88	0.46	0.26
SBF [1]	20.4	18.3	16.7	15.3	0.88	0.83	0.77	0.70
NLM [17]	27.0	20.0	17.1	15.8	0.93	0.87	0.82	0.78
OBANLM [31]	28.1	21.9	19.4	17.1	0.94	0.92	0.85	0.80
NLMLS [29]	29.0	23.2	20.3	18.3	0.96	0.93	0.87	0.85
Proposed	31.0	24.1	20.8	18.3	0.97	0.94	0.88	0.85

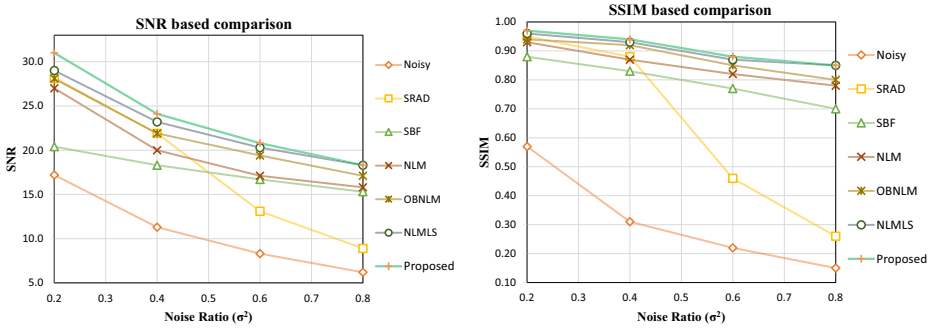


Fig. 4 Performance of different denoising filters on synthetic images at different speckle noise ratios

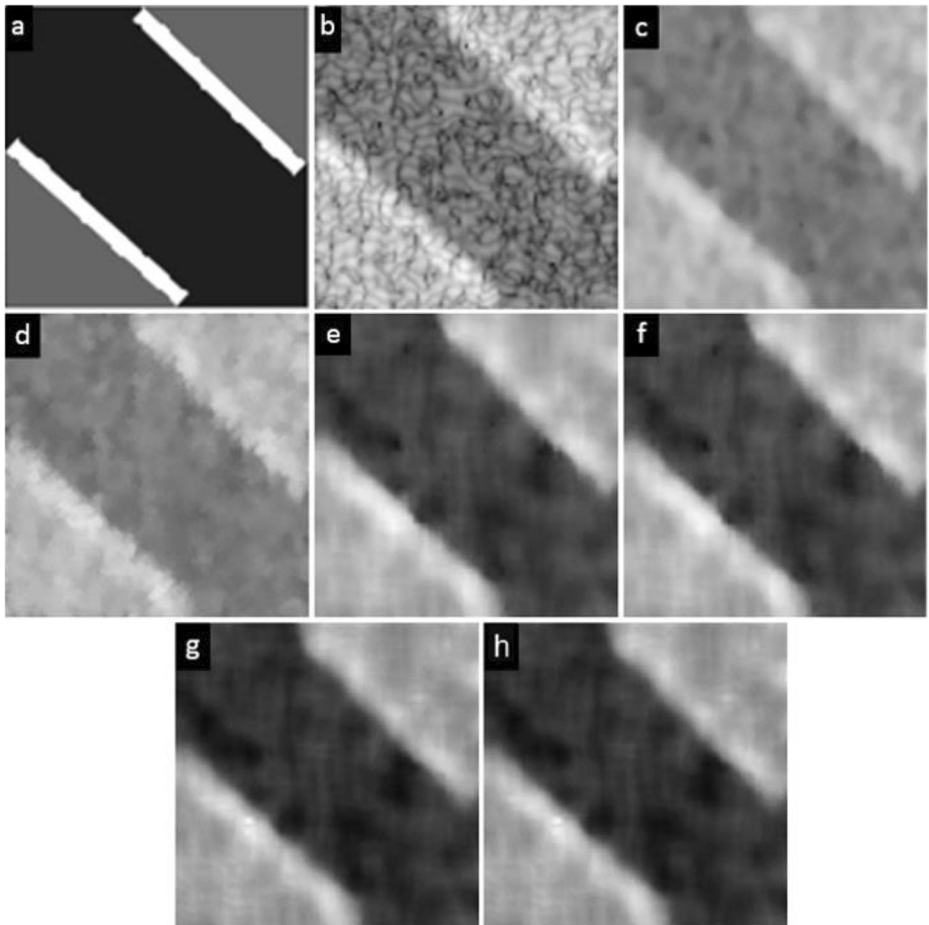


Fig. 5 Results of Experiment-II (B-mode simulated image): a Original image b image with speckle noise c SRAD d SBF e NLM f OBFLM g NLMLS h Proposed filter

### 3.2 B-mode ultrasonic simulated images (Experiment-II)

The effectiveness of different state of the art despeckled filters and proposed filter is observed by conducting experimentation on B-mode ultrasonic images. The B-mode simulated image [3] is different from the synthetic image in terms of background which shows different kind of features shown in Fig. 5a. The noisy B-mode simulated image possessing the features of B-scan images is generated in MATLAB by setting multiple parameters. These are: center frequency of the ultrasonic wave is kept 10e6, velocity of sound in media is set to 1540 m/s, variance of speckle noise distribution in image is set to 0.01, pulse-width of the transmitter is 2 mm and beam width is set to 1.5 mm. Original and simulated ultrasound image is shown in Fig. 5a and b. The size of the image is kept  $128 \times 128$  and is log-compressed for displaying purpose.

Multiple regions shown in the image are regarded as different tissues. Fig. 5b presents noisy speckled image with  $\sigma = 0.6$  and Fig. 5c-h shows the reconstructed images after applying SRAD, SBF, NLM, OBNLM, NLMLS and proposed filters. It is noticeably seen from the restored images obtained after applying these filters that the performance shown is quite unsatisfactory. Moreover, due to iterative nature of SRAD and SBF filters, they show negative influence on contrast. The performance of NLMLS and the proposed filter in terms of speckle reduction is very remarkable. But in terms of edge preservation, NLMLS has less accuracy as compared to the proposed filter. The regions in Fig. 5h are more uniform and close to the original image, edges are more preserved compared to Fig. 5g which produces blurred edges in the image.

The quantitative values of SNR and SSIM listed in Table 2 verifies the best performance of the proposed filter in despeckling B-mode ultrasound images. SNR shows that proposed technique outperforms and SSIM shows that it is almost same as that of NLMLS and OBNLM.

### 3.3 Field II kidney simulation (Experiment-III)

In this experiment, performance of the proposed despeckling filter is evaluated on simulated kidney ultrasonic image generated through linear acoustics and Field II program provided by J. A. Jenson [13, 14, 30]. This program uses Tophole-Stepanishen method to evaluate pulsed ultrasound fields. The kidney data set is more challenging because of the lack of regularly shaped region. Fig. 5 shows the comparison of the existing and proposed filters on Field II kidney simulated image. Fig. 6a and b shows the original and noisy image with  $\sigma = 0.4$ . Fig. 6c-h shows the reconstructed images after applying SRAD, SBF, NLM, OBNLM, NLMLS and proposed filters respectively. Visual inspection of the results reveal that the SRAD, SBF,

**Table 2** Comparison of SNR (db) and SSIM of different denoising filters on B-mode simulated images contaminated with different levels of speckle noise (Experiment-II)

Method	SNR	SSIM
Noisy image	5.58	0.11
SRAD [35]	5.68	0.33
SBF [31]	5.55	0.33
NLM [6]	5.65	0.37
OBNLM [8]	5.65	0.38
NLMLS [34]	5.67	0.38
Proposed	9.24	0.38

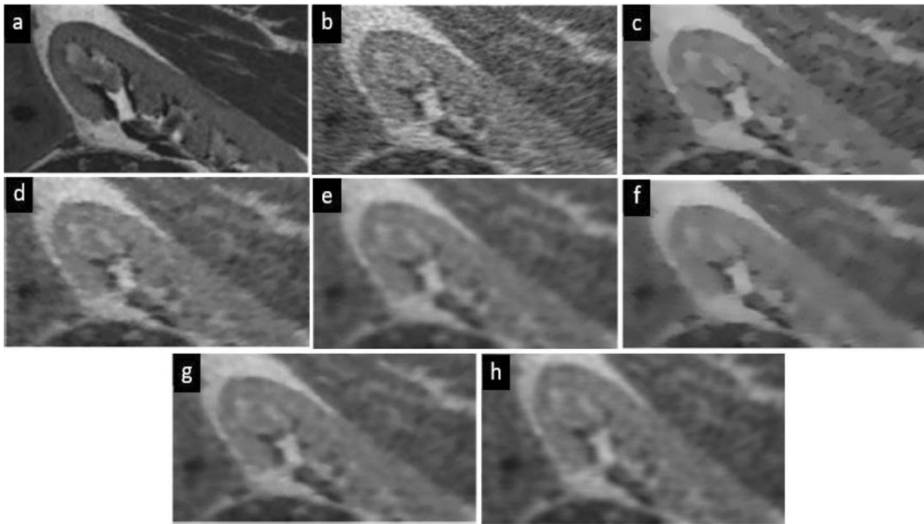


**Fig. 6** Results of Experiment-III (Field II simulated images): **a** Original image **b** Speckled image **c** SRAD **d** SBF **e** NLM **f** OBNLM **g** NLMLS **h** Proposed filter

NLM and OBNLM filters tends to over smooth the image; NLMLS and proposed filter produce significant results but Fig. 6h seems to be more uniform, sharper and retains more fine texture, which proves the best performance of the proposed filter.

The numerical values of SNR and SSIM produced by the comparative and proposed filters are listed in Table 3. The high values of SNR and SSIM obtained by proposed filter (16.59db and 0.54) indicates its superiority over other comparative filters in terms of speckle noise reduction and fine structure preservation capabilities.

### 3.4 Real ultrasound images (Experiment-IV)

Filtering the real ultrasound images and evaluating qualitatively is a challenging task because of the characteristics of the acquired signal. Extensive experimentation is performed on the real images of liver, urinary tract downloaded from “[www.ultrasoundcases.info](http://www.ultrasoundcases.info)”. For evaluating the performance of the proposed filter, a sample speckled image of liver and the reconstructed images after applying SRAD, SBF, NLM, OBNLM and proposed filters are shown in Fig. 7. Visual inspection of the results reveals that the SRAD, SBF and NLM filters shown in Fig. 7b-

**Table 3** Comparison of SNR (db) and SSIM of different denoising filters on Field II simulated images contaminated with different levels of speckle noise (Experiment-III)

Method	SNR	SSIM
Noisy image	8.53	0.12
SRAD [35]	9.41	0.45
SBF [31]	9.12	0.42
NLM [6]	9.51	0.50
OBNLM [8]	9.51	0.50
NLMLS [34]	9.60	0.50
Proposed	16.59	0.54

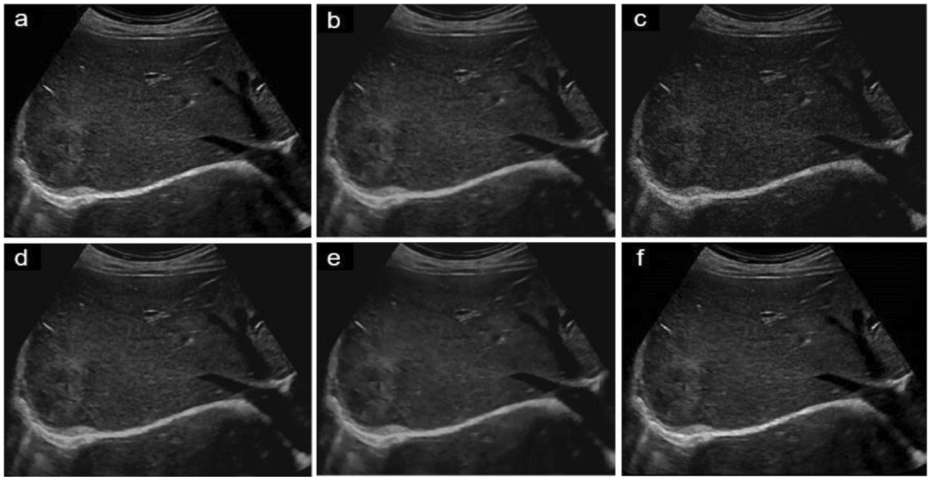


**Fig. 7** Results of Experiment-IV (real image): **a** Speckled image **b** SRAD **c** SBF **d** NLM **e** OBNNM **f** Proposed filter

**d** preserves the details but does not remove much noise from the images. OBNNM filter shown in Fig. 7e removes noise considerably but tends to over smooth the image. Additionally OBNNM takes long processing time for large size ultrasonic images. Proposed filter produce outstanding results as shown in Fig. 7f and seems to be more uniform, sharp and retains more fine structural details in small areas of the image.

## 4 Conclusions

In the study, a novel fuzzy NLM-based filter is proposed for denoising highly speckled ultrasonic images effectively by integrating local and non-local statistical information to figure out the degree of similarity of different regions. The proposed filter not only suppresses the speckle noise considerably but also preserves the fine details and other small structures present in an the image in a better way than other speckle reduced filters. Various experiments are conducted on synthetic, simulated and real images to verify the fact. The images are synthesized with different levels of simulated speckle noise. Quantitative and qualitative evaluations are provided to compare the proposed technique with numerous state of the art filters used for despeckling ultrasound images. The quantitative analysis of the experimental results verify that the proposed filter exhibits the best despeckling performance in terms of SNR and SSIM values. The human visual assessment suggests that the proposed filter preserves the fine detail and edges present in the small areas of lesions while removing the speckle noise effectively as compared to other state of the art filtering techniques. In future, we aim to improve the noise reduction performance of the proposed algorithm so that it can be used in real time scenario to assist doctors in analysis and interpretation of ultrasonic images.

**Publisher's note** Springer Nature remains neutral with regard to jurisdictional claims in published maps and institutional affiliations.

## References

1. Abd-Elmoniem KZ, Youssef A, Kadah YM (2002) Real-time speckle reduction and coherence enhancement in ultrasound imaging via nonlinear anisotropic diffusion. *IEEE Trans Biomed Eng* 49(9):997–1014
2. Ambrosanio M, Baselice F, Ferraioli G, Pascasio V (2018) Ultrasound despeckling based on non local means. In: Eskola H, Väisänen O, Viik J, Hyttinen J (eds) *EMBECE & NBC 2017*. *EMBECE 2017, NBC 2017*. *IFMBE Proceedings*, vol. 65. Springer
3. Bamber JC, Dickinson RJ (1980) Ultrasonic B-scanning: a computer simulation. *Phys Med Biol* 25(3)
4. Baselice F (2017) Ultrasound Image Despeckling Based On Statistical Similarity. *Ultrasound Med Biol*, Elsevier 43(9):2065–2078
5. Binaee K, Hasanzadeh RPR (2011) A non local means method using fuzzy similarity criteria for restoration of ultrasound images. In: 7th Iranian Conference on Machine Vision and Image Processing (MVIP), Tehran, pp. 1–5
6. Buades A, Coll B, Morel J (2005) A non-local algorithm for image denoising. In: *IEEE Computer Society Conference on Computer Vision and Pattern Recognition (CVPR'05)*, San Diego, vol. 2, pp. 60–65
7. Chen Y, Broschat SL, Flynn PJ (1996) Phase insensitive homomorphic image processing for speckle reduction. *Ultrasound Imaging* 18(2):122–139
8. Coupe P, Hellier P, Kervrann C, Barillot C (2009) Nonlocal means-based speckle filtering for ultrasound images. *IEEE Trans Image Process* 18(10):2221–2229
9. Frost VS, Stiles JA, Shanmugan KS, Holtzman JC (1982) A Model for Radar Images and Its Application to Adaptive Digital Filtering of Multiplicative Noise. *IEEE Trans Pattern Anal Mach Intell PAMI-4(2)*:157–166
10. Ghesu FC, Georgescu B, Zheng Y, Grbic S, Maier A, Hornegger J, Comaniciu D (2017) Multi-scale Deep Reinforcement Learning for Real-Time 3D-Landmark Detection in CT Scans. *IEEE Transactions on Pattern Analysis and Machine Intelligence*
11. Gonzalez RC, Woods RE (2004) *Digital Image Process*. Pearson Education (Singapore) Pte. Ltd, Delhi
12. Javed SG, Majid A, Lee YS (2017) Developing a bio-inspired multi-gene genetic programming based intelligent estimator to reduce speckle noise from ultrasound images. *Multimedia Tools Appl*
13. Jensen JA (1996) Field: a program for simulating ultrasound systems. Paper presented at the 10th Nordic-Baltic Conference on Biomedical Imaging
14. Jensen JA, Svendsen NB (1992) Calculation of pressure fields from arbitrarily shaped, apodized, and excited ultrasound transducers. *IEEE Transactions on Ultrasonic, Ferroelectrics, and Frequency Control* 39(2):262–267
15. Ker J, Wang L, Rao J, Lim T (2018) Deep Learning Applications in Medical Image Analysis. *IEEE Access* 6:9375–9389
16. Kim J, Hong J, Park H (2018) Prospects of deep learning for medical imaging. *Precision and Future Medicine* 2:37–52
17. Krissian K, Westin C, Kikinis R, Vosburgh KG (2007) Oriented Speckle Reducing Anisotropic Diffusion. *IEEE Trans Image Process* 16(5):1412–1424
18. Kuan DT, Sawchuk AA, Strand TC, Chavel P (1985) Adaptive Noise Smoothing Filter for Images with Signal-Dependent Noise. *IEEE Trans Pattern Anal Mach Intell PAMI-7(2)*:165–177
19. Lan X, Ye M, Zhang S, Yuen PC (2018) Robust Collaborative Discriminative Learning for RGB-Infrared Tracking. In: *AAAI Conference on Artificial Intelligence, North America*. Date accessed: 21 Nov. 2018
20. Lan X, Yuen PC, Chellappa R (2017) Robust MIL-based feature template learning for object tracking. In: *AAAI Conference on Artificial Intelligence, North America*. Date accessed: 21 Nov. 2018
21. Lan X, Zhang S, Yuen PC, Chellappa R (2018) Learning Common and Feature-Specific Patterns: A Novel Multiple-Sparse-Representation-Based Tracker. *IEEE Trans Image Process* 27(4):2022–2037
22. Lee J (1980) Digital Image Enhancement and Noise Filtering by Use of Local Statistics. *IEEE Trans Pattern Anal Mach Intell PAMI-2(2)*:165–168
23. Lu L, Zheng Y, Carneiro G, Yang L (2017) *Deep learning and convolutional neural networks for medical image computing*. Springer
24. Maier A, Syben C, Lasser T, Riess C (2018) A gentle introduction to deep learning in medical image processing. [arXiv:1810.05401v1](https://arxiv.org/abs/1810.05401v1)
25. Masood S, Hussain A, Arfan Jaffar M, Choi T-S (2014) Color differences based fuzzy filter for extremely corrupted color images. *Appl Soft Comput* 21:107–118, ISSN 1568-4946
26. Chaudary A, Khan A, Mirza AM, Ali A (2007) A Hybrid Image Restoration Approach: Using Fuzzy Punctual Kriging based Image Restoration. *Int J Imaging Syst Technol* 17(4):224–231



27. Nirschl JJ, Janowczyk A, Peyster EG, Frank R, Margulies KB, Feldman MD, Madabhushi A (2017) Deep learning tissue segmentation in cardiac histopathology images. In: *Deep Learning for Medical Image Analysis*, Elsevier, pp. 179–195
28. Sharif M, Ayyaz Hussain M, Arfan J, Choi T-S (2015) Fuzzy similarity based Non Local Means Filter for Rician Noise Removal. *Multimed Tools Appl* 74(15):5533–5556
29. Sharif M, Hussain A, Jaffar MA, Choi TS (2016) Fuzzy-based hybrid filter for rician noise removal. *SIViP* 12:215–224
30. Singh K, Ranade SK, Singh C (2017) A hybrid algorithm for speckle noise reduction of ultrasound images. *Comput Methods Prog Biomed* 148:55–69
31. Tay PC, Garson CD, Acton ST, Hossack JA (2010) Ultrasound Despeckling for Contrast Enhancement. *IEEE Trans Image Process* 19(7):1847–1860
32. Wang Z, Bovik AC, Sheikh HR, Simoncelli EP (2004) Image quality assessment: from error visibility to structural similarity. *IEEE Trans Image Process* 13(4):600–612
33. Wu J, Tang C (2014) Random-valued impulse noise removal using fuzzy weighted non-local means. *Signal, Image Video Processing* 8(2):349–355
34. Yang J, Fan J, Ai D, Wang X, Zheng Y, Tang S, Wang Y (2016) Local statistics and non-local mean filter for speckle noise reduction in medical ultrasound image. *Neurocomputing* 195:88–95
35. Yu Y, Acton ST (2002) Speckle reducing anisotropic diffusion. *IEEE Trans Image Process* 11(11):1260–1270
36. Zhang K, Zuo W, Chen Y, Meng D, Zhang L (2017) Beyond a Gaussian Denoiser: Residual Learning of Deep CNN for Image Denoising. *IEEE Trans Image Process* 26(7):3142–3155



**Muhammad Nadeem** has received his MS degree in computer science in 2007 from International Islamic University, Islamabad, Pakistan. He is pursuing his Ph.D. research at the Department of Computer Science & Software Engineering, IIU Islamabad, Pakistan and currently he has been working as an Assistant Professor in the same department. His research interests include computer vision, medical image processing, machine learning and computational intelligence.



**Ayyaz Hussain** has received his B.Sc. degree from Punjab University Lahore. He later received M.Sc. degree in computer science, in 2000, from Quaid-e-Azam University Islamabad, Pakistan. Then he earned his PhD degree in computer science in 2009 from National University of Computer and Emerging Sciences, NUFAST, Islamabad, Pakistan. He has been working as an Associate Professor at the Department of Computer Science & Software Engineering, IIU Islamabad, Pakistan since August 2010. His research interests include image processing, machine learning and computational intelligence.



**Asim Munir** has received his MS degree in computer science in 2006 from International Islamic University, Islamabad, Pakistan. He is pursuing his Ph.D. research at the Department of Computer Science & Software Engineering, IIU Islamabad, Pakistan and currently he has been working as an Assistant Professor in the same department. His research interests include computer vision, medical image processing, machine learning and computational intelligence.